A complementary switching mechanism for organic memory devices to regulate the conductance of binary states

Giriraj Vyas, Parveen Dagar, and Satyajit Sahu

Citation: Appl. Phys. Lett. **108**, 233301 (2016); doi: 10.1063/1.4953197
View online: http://dx.doi.org/10.1063/1.4953197
View Table of Contents: http://aip.scitation.org/toc/apl/108/23
Published by the American Institute of Physics

A complementary switching mechanism for organic memory devices to regulate the conductance of binary states

Giriraj Vyas, Parveen Dagar, and Satyajit Sahu[a)]
Department of Physics, Indian Institute of Technology Jodhpur, Jodhpur, Rajasthan 342011, India

(Received 9 March 2016; accepted 21 May 2016; published online 6 June 2016)

We have fabricated an organic non-volatile memory device wherein the ON/OFF current ratio has been controlled by varying the concentration of a small organic molecule, 2,3-Dichloro-5,6-dicyano-*p*-benzoquinone (DDQ), in an insulating matrix of a polymer Poly(4-vinylphenol) (PVP). A maximum ON-OFF ratio of 10^6 is obtained when the concentration of DDQ is half or 10 wt. % of PVP. In this process, the switching direction for the devices has also been altered, indicating the disparity in conduction mechanism. Conduction due to metal filament formation through the active material and the voltage dependent conformational change of the organic molecule seem to be the motivation behind the gradual change in the switching direction. *Published by AIP Publishing.*
[http://dx.doi.org/10.1063/1.4953197]

Organic electronic devices have created a niche of their own by commercially producing devices such as Organic Light Emitting Diode (OLED),[1] Organic Field Effect Transistor (OFET),[2] and organic solar cell.[3] The reasons making them more useful are the flexibility of fabrication,[4] less cost,[5] solution processability,[6] and facile synthesis of the active material. For these devices, the performance is comparable with their inorganic counterparts. There are some organic electronic devices which show promise, but because of the lack of general understanding of their operation, they are yet to be commercialized. One such device is the organic memory device. Memory devices have a fair share in the electronic market, and the majority of them are dynamic random access memory devices (DRAM). Flash memory devices, such as a solid state drive, are available in the market but are very expensive. Silicon based devices are limited by the size on the crystalline substrates, but this limitation can be overcome by using organic memory devices in which a single molecule will be used as the switching device.[7]

Traditionally, the switching behaviour of the resistive devices has been explained in many ways, and few of the major mechanisms that have been adopted are, namely, conformational change of the molecule[8] in the active material, charge retention in the organic matrix,[9] and conducting metal filament formation through the active layer.[10] Recent development in this field has again put the attention back on the operation mechanism of memory device wherein it is strongly suggesting that the charge transfer complex (CTC) formation and conformational state of the molecule is responsible for the switching in the devices.[11] Here, we have tried to show that both formation of filament and conformational change of the molecule are responsible for the switching between conducting states in these devices. The concentration of organic molecule in the insulating polymer matrix dictates the mechanism responsible for switching. The ON/OFF ratio of the binary states for the device can be controlled by adding suitable functional groups[12] or by using composite of organic and inorganic materials.[13] Here, we have tuned the ON/OFF ratio by controlling the ratio of the insulating polymer and the small organic molecule.

The substrate used for the device fabrication was indium tin oxide (ITO). Standard cleaning procedure was followed to clean the substrate, i.e., the substrates were first cleaned in soap solution using ultrasonicator followed by rinsing in deionized (DI) water. Then, these substrates were cleaned in acetone, DI water, and methanol thrice for each solvent, using an ultrasonicator. The cleaned substrates were dried in a vacuum oven at 70 °C for a few hours. The active materials being used for the devices are 2,3-Dichloro-5,6-dicyano-*p*-benzoquinone (DDQ) and Poly(4-vinylphenol) (PVP). All the materials are procured from Aldrich, Co., and used without further purification. The solution for both the materials was prepared using Isopropyl alcohol (IPA). The solution concentration for the deposition of films was varied with respect to the volume concentration of DDQ. It was varied as the weight ratio of DDQ in PVP increased from 5% to 30% with an increment of 5% and another composition having 50% weight ratio of DDQ in PVP. Once the solutions were ready, the spin coated films were deposited on the substrates at 7400 RPM. The films thus deposited were dried in vacuum at room temperature for at least 12–14 h. The thickness measurements were carried out using Bruker Dektak XT-100 profilometer, and the average thickness was calculated to be 174 nm. Since the films are deposited on a striped conducting surface (ITO), the ITO acts as a bottom contact. A 70 nm thick Aluminium (Al) layer was thermally evaporated on top of the films, which acts as the top contact for the device. Once ready, the devices were characterized in vacuum using a 2 probe measurement technique by using a Keithley 6430 femto-ampere source meter. The absorbance of the solution for individual as well as combined components was recorded by using Agilent Cary 4000 UV VIS spectrometer.

The molecular structure of the materials used for device fabrication is shown in Figure 1(a). The absorbance spectra of DDQ mixed in PVP, which is shown in Figure 1(b), are studied carefully, and the absorbance peak for DDQ in IPA

a)Author to whom correspondence should be addressed. Electronic mail: satyajit@iitj.ac.in

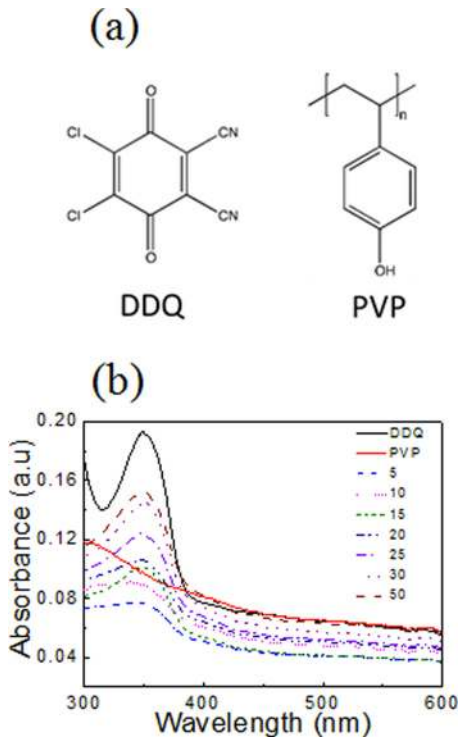

FIG. 1. (a) Molecular structure of DDQ and PVP. (b) Absorption spectra of pristine DDQ, PVP, and a mixture of both at various concentrations (5% to 30% of DDQ in PVP at a difference of 5% and 50% DDQ in PVP) in a common solvent. (b)–(d) Topographic AFM images of the thin films of the mixture of PVP and DDQ at weight ratio of 5%, 10%, and 15%, respectively. The scale bar is representing a length scale of 1 μm for all the images. The scanned area is 5 × 5 μm^2. The arrows in (b) indicate the pin holes within the drawn circle (red).

is obtained at 349 nm, and for PVP, the absorbance peak is obtained in the UV region. As the weight ratio for DDQ keeps increasing in the combined solution of PVP and DDQ, it is found that the absorption peak for DDQ is increasing proportionally. There is no hint on the formation of charge transfer complex (CTC), as there is no appearance of new peaks due to formation of CTC. We also carried out the absorbance study on thin films and found that there is no formation of charge transfer complex in the solid films of the materials.

The topography of all the films is studied by using a Park System XE 70 atomic force microscope in the non-contact mode. A minimum scan rate of 0.25 nm^2/s was maintained to obtain the highest resolution images for the topography of the surface. All the films used for taking AFM images were fabricated under the same conditions as those used for the device. From the topographic images of all the devices, it is found that despite all the films being rough, there are pinholes on the surface as indicated by the arrows inside the circle in Figure 2(d). The size and number of the pinholes vary across the devices. It is found that for the device having 5% weight ratio of DDQ (Figure 2(a)), the total number of pinholes is 231 and the pinhole size varies from 20–120 nm. For other devices, the number of pinholes and the size vary as follows: devices with 10% weight ratio have 430 number of pin holes in the range of 35–85 nm (Figure 2(b)); for 15% devices, it is 586 in number spanning in the range of 25–90 nm (Figure 2(c)); for 20% devices, it is 438 in number in the range of 30–100 nm (Figure 2(d)); for 25%, it is 430 in number having hole size in the range of 20–55 nm (Figure 2(e)); for 30% device, it is 426 in number having hole size in the range of 30–95 nm (Figure 2(f)); and for the 50% device, it is 532 in number having hole size in the range of 25–85 nm (Figure 2(g)). It is observed that there is an oscillation in the number of pinholes with respect to the concentration. The reason for this oscillation is still under investigation.

The device structure studied in this work are as follows: the weight ratio of DDQ is 5%, 10%, 15%, 20%, 25%, 30%, and 50% of PVP. The labels assigned for these devices are *A, B, C, D, E, F,* and *G,* respectively.

The I-V curves for the devices were obtained by scanning the devices at a scan rate of 50 mV/s. As shown in Figure 3(a) for *device A*, in the positive scan of the device, the difference of current in the low (OFF) and high (ON) conducting states is high, whereas when the device traces in the negative bias direction, there is a small difference in the current for the ON and OFF states. The highest ON/OFF ratio obtained for the device in the negative direction is 5, which is significantly less to be used as a memory device, whereas the ON/OFF ratio in the positive direction is 32. The voltage range has also been varied to a maximum of 4 V, but every time the feature remained same with a varying ON/OFF ratio.

For *device B*, in the negative scan, the maximum ON/OFF ratio that is achieved is of the order of 10^6 as seen from the inset of Figure 3(b). The IV curve is smoother than *device A*, which indicates that the transport is becoming better by the formation of concrete conducting filament pathways. The maximum ON/OFF ratio that is obtained for *device C* in the negative direction is 150. In the positive voltage scan, there is no bistability observed. The ON/OFF ratio has drastically reduced in comparison to the previous two devices as can be observed from Figure 3(c). The maximum ON/OFF ratio for *device D* in Figure 3(d) is of the order of 20 in the negative voltage scan. Statistically, the devices show an invariable transport in most of the cells, suggesting the formation of strong insulating pathways that does not allow smooth transport of charge carriers.

The IV curve for *device E* is not smooth, and the ON/OFF ratio for them is not very high as it only reached to 23 in the negative scan and 135 in the positive voltage scan, as is shown in Figure 3(e). The current density for the device is much smaller than that for the previous devices. Statistically, most of the devices showed a very sluggish transport, and hence, the ON/OFF ratio is also affected. The hint on space-charge accumulation is an indication of the signature of hysteresis in the devices. There are some devices which showed switching in the positive direction consistently though the percentage is less in comparison to the devices which do not show any switching behaviour (14%, i.e., 9 out of 61 times), which is an indication that DDQ is now the dominating factor for the switching in the devices.

The highest ON/OFF ratio for *device F* is of the order of 10 in the negative voltage scan whereas it is of the order of 10^4 in the positive direction, as can be seen from Figure 3(f). For *device G* in Figure 3(g), in the negative voltage scan, the current hardly had any difference in the ON and OFF states. In the positive scan, the difference in current between the

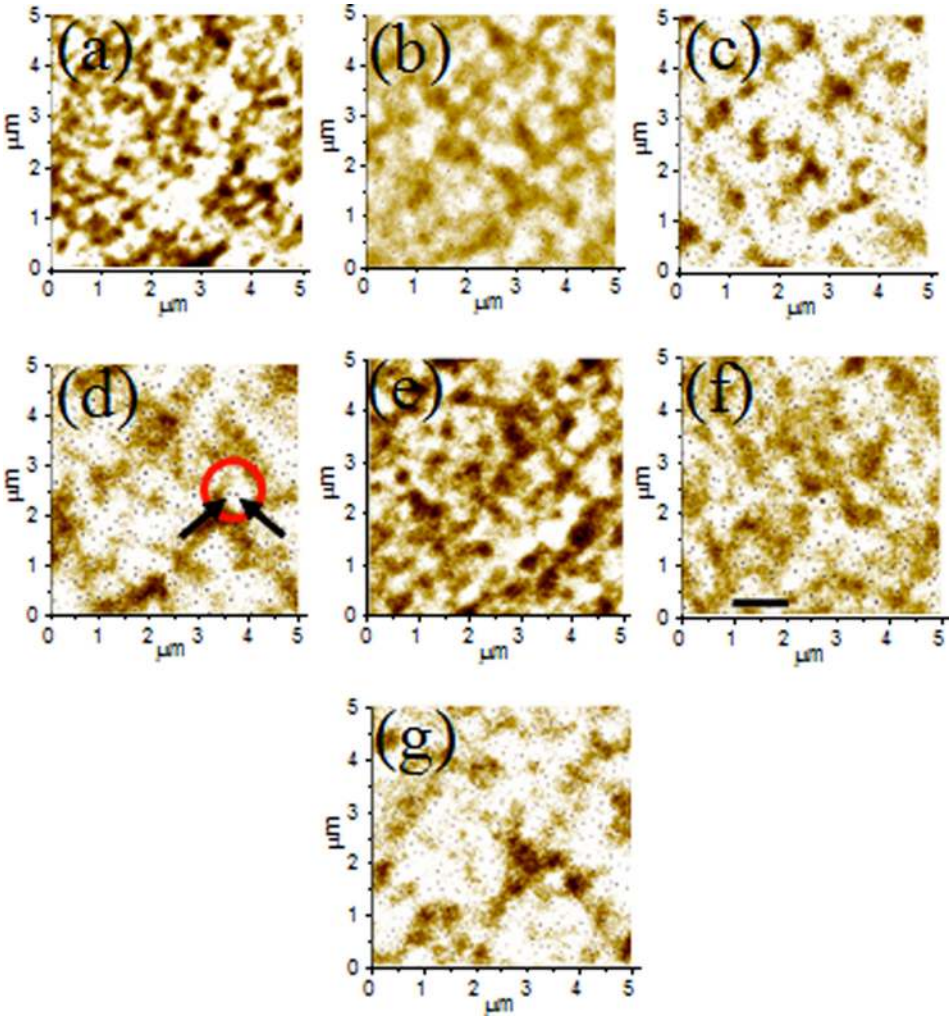

FIG. 2. (a)–(g) Topographic AFM images of the thin films of the mixture of PVP and DDQ at weight ratios of 5%, 10%, 15%, 20%, 25%, 30%, and 50%, respectively. The scale bar represents a length scale of 1 μm. The scanned area is 5 × 5 μm^2. The arrows in (d) indicate the pin holes within the drawn circle.

ON and the OFF states is of the order of 10^6, which is much higher than the previous two (*E* and *F*) devices. The devices in this composition showed reproducibility in multiple scans.

From all the devices' configuration, one thing is very clear, that is, the switching from OFF state to ON state started on the negative scan of voltage with a very less ON/OFF ratio and then reached to a higher value and eventually came down to a very low value with a complete shift in the switching in the positive scan of voltage. Inherently switching in only the DDQ based devices is restricted in the positive side of the voltage scan for a spin coated sandwiched device structure.[12] But the switching in the negative side of voltage scan suggests the formation of metal filament due to electromigration of Al through the pinholes on the surface of the film,[14,15] and as soon as the Al ions were forced to move under the external electric field, the conduction starts becoming better, and when the contact with the bottom electrode is made, the conductance jumps to a very high value, as shown in the schematic of Figure 4(a), block 1 to 3. This is also experimentally verified by Infrared (IR) imaging of the devices during the negative voltage scan. Sometimes, it is observed that the switching is independent of the organic matrix.[15] It can be said that because of the low concentration, the pinholes are partially filled with the DDQ molecules. Hence, the formation of filament is the only reason for switching in the less concentrated DDQ based devices. As the concentration increases, the pinholes mainly constitute DDQ, and the switching in these devices is primarily due to DDQ; consequently, the ON-OFF ratio also increases in orders of magnitude as can be seen from Figure 4(c), blocks 4 and 5. Since PVP is an insulator, the band gap for the material must be very large in comparison to DDQ; hence, the interaction between Al with PVP propels the Al ions to form the filament in such a way that the switching direction follows the negative bias of the applied voltage, whereas the interaction between DDQ and Al shifted the switching to the positive direction as in higher concentration films, DDQ covers most part of the pinholes, and the pinholes are also shallow, which allow little formation of Al filament through the pinholes and hence no switching of conductivity in the negative direction. Moreover, when a negative bias is applied, DDQ undergoes reduction by capturing all the electrons drifting through the Al channels by the electronegative oxygen atoms and it releases the electron when a suitable positive bias is applied, and hence, there is a jump in conductivity in the positive voltage scan.[12]

All the devices can be used as non-volatile memory device as they showed both the properties of Random Access Memory (RAM) and Read Only Memory (ROM). To test the RAM application of the devices, they were scanned by a write voltage pulse for some time and then probed with a read voltage pulse followed by an erase voltage and again a

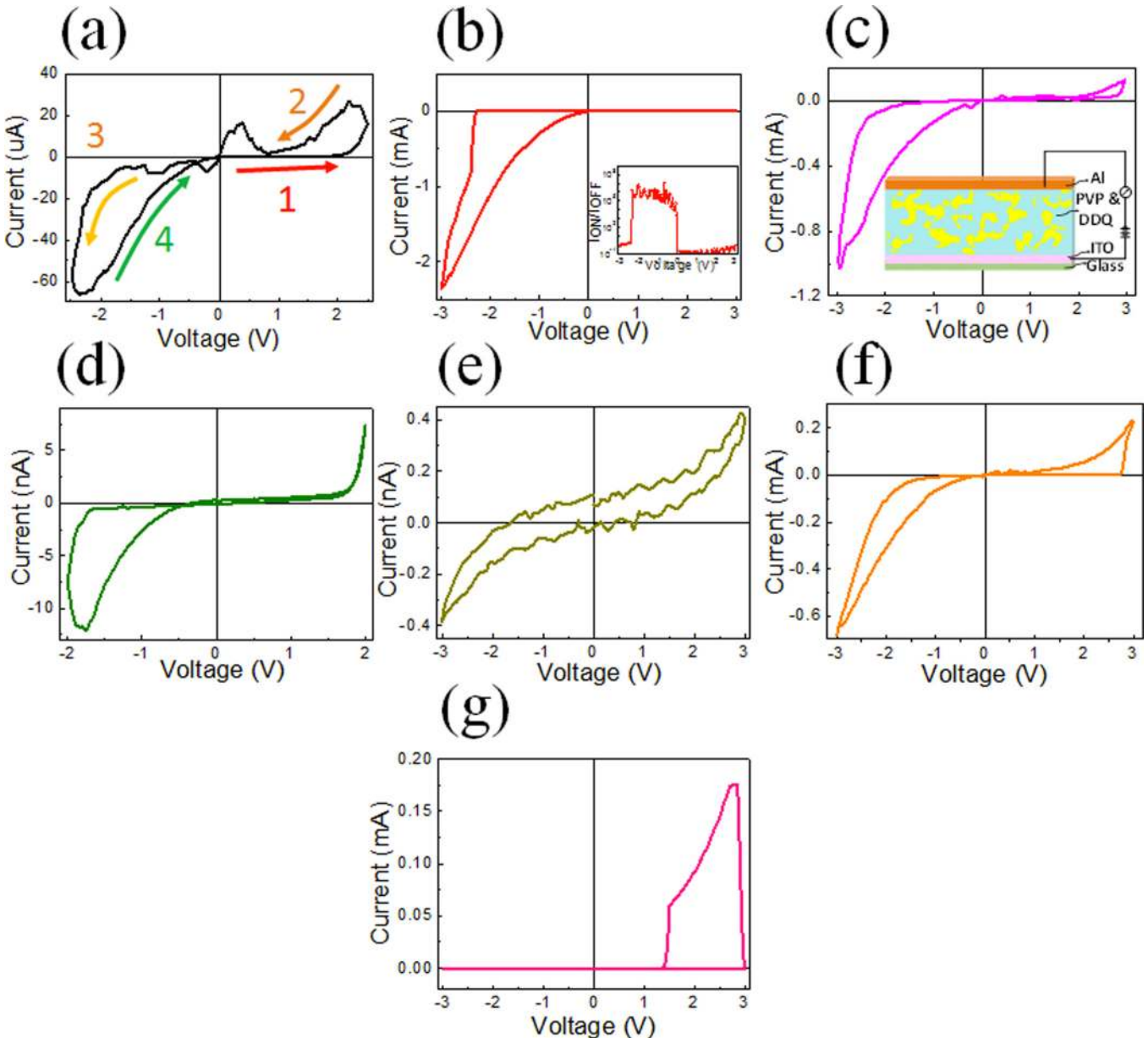

FIG. 3. (a) IV characteristic curve of *device A*. The numbered (1 to 4) arrows (red, orange, yellow, and green) are representing the order of the scanning direction. (b) and (c) IV characteristic curves for *devices B* and *C*, which are scanned from 3 to −3 V. The inset of (b) shows the ON/OFF ratio for the device within the spectrum of the above voltage scan. The inset of (c) shows the device structure where the legends read as follows: Aluminium (Al), the active layer (PVP & DDQ), Indium Tin Oxide (ITO), and glass. (d)–(g) The IV characteristic curves of *devices D, E, F,* and *G*. There is shift in the switching direction through the decrease in current and then increase in the current at higher concentration of DDQ.

read voltage pulse. The train of Write-Read-Erase-Read voltage pulse sequence is applied for a number of cycles to test the reliability of the devices. In Figure 4(b), we have shown the scan for RAM for a device where the write voltage (V_{write}) is −3 V, the erase voltage (V_{erase})is +3 V, and the read voltage (V_{read}) is −0.5 V. The write and erase voltage pulse were applied for 5 s each, whereas the read pulse was applied for 20 s after every write and erase pulse. We have applied this sequence for 1000 s or for 20 times and found that the device shows stability towards retention of memory. The current level in the read pulses does not change significantly, which hints the stability even during the random probe of the devices.

For the study of read only memory, the devices have been probed using a small read voltage pulse following a write or erase voltage. The write voltage is applied at −3 V, and the corresponding erase voltage is 3 V. To probe the device, a voltage pulse of −0.5 V is used for more than 1000 s and is found to be reasonably stable in the whole period of probe voltage. So, both the RAM and ROM application can be shown in all the devices having different concentrations of DDQ in PVP. The ON/OFF ratio matches with the ON/OFF ratio obtained in case of Write-Read-Erase-Read sequence.

In conclusion, the non-volatile memory devices have been fabricated using a combination of semiconducting organic molecule and an insulating polymer. The ON/OFF ratio for the device can be controlled by varying the weight ratio of PVP and DDQ in the mixture. The conductance ratio is high when the proportion of DDQ is either very less or

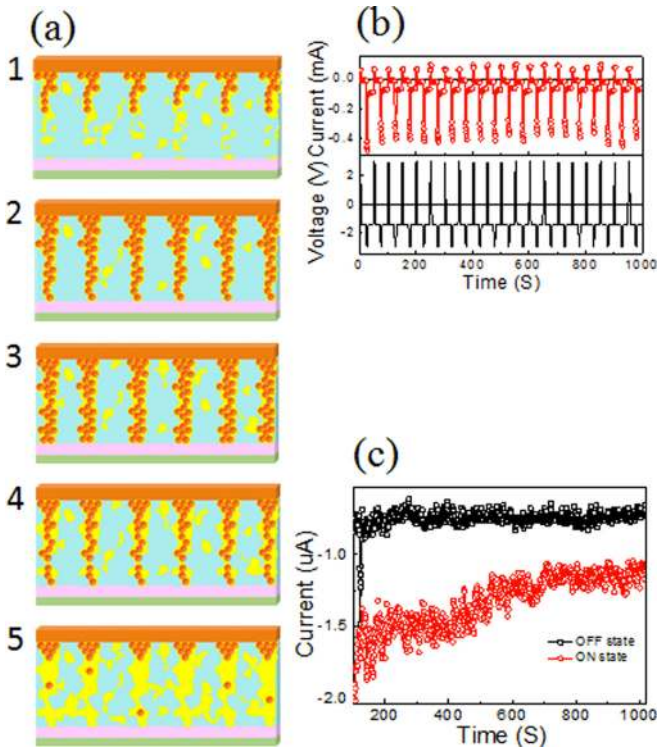

FIG. 4. (a) Schematic of conduction mechanism in the devices starting with the formation of seed for the metal filament at a low DDQ concentration to the conformational change of DDQ in the mixture. The yellow region represents parts of DDQ, the light blue region is PVP matrix, and the orange colour balls represent Al ions. (b) The write-read-erase-read sequence to test the consistency of reading the written state which are written at −3 V for 5 s, and erased at 3 V for 5 s, and after writing and erasing, the states are read at 0.5 V for 5 s each for 4 times. The cycle was continued for 1000 s. (c) After writing and erasing by −3 V (ON state) and 3 V (OFF state), the states are read for 1000 s to test the stability of the devices with continuous probing at −0.5 V.

equal to half of that of PVP. When the concentration of PVP is more, the bistability is observed in the negative voltage bias, and when the ratio of DDQ and PVP is half, the difference in conductance is prominent in the positive direction. This feature was explained by using the model of conducting metal filament formation and voltage dependent conformational change of the organic molecule, respectively. Both the mechanisms were validated from the observation of formation of varied sizes of pinholes on the surface of the thin films. Thus, the switching ratio and direction can be controlled by varying the concentration of semiconductor in insulating matrix.

This work was supported by Department of Science and Technology (DST) through INSPIRE Faculty Program with Project No. IFA12-PH-26. The authors are thankful to IIT Jodhpur for providing all the support.

[1]C. W. Tang and S. A. VanSlyke, Appl. Phys. Lett. **51**(12), 913 (1987).
[2]G. Horowitz, Adv. Mater. **10**(5), 365 (1998).
[3]C. W. Tang, Appl. Phys. Lett. **48**(2), 183 (1986).
[4]T. F. O'Connor, A. V. Zaretski, S. Savagatrup, A. D. Printz, C. D. Wilkes, M. I. Diaz, E. J. Sawyer, and D. J. Lipomi, Sol. Energy Mater. Sol. Cells **144**, 438 (2016).
[5]S. R. Forrest, Nature **428**(6986), 911 (2004).
[6]K. C. Dickey, J. E. Anthony, and Y. L. Loo, Adv. Mater. **18**(13), 1721 (2006).
[7]J. Chen, M. A. Reed, A. M. Rawlett, and J. M. Tour, Science **286**(5444), 1550 (1999).
[8]A. Bandhopadhyay and A. J. Pal, Appl. Phys. Lett. **84**(6), 999 (2004).
[9]J. C. Scott and L. D. Bozano, Adv. Mater. **19**(11), 1452 (2007); S. Gao, C. Song, C. Chen, F. Zeng, and F. Pan, J. Phys. Chem. C **116**(33), 17955 (2012).
[10]M. Cölle, M. Büchel, and D. M. de Leeuw, Org. Electron. **7**(5), 305 (2006).
[11]Q. Zhang, J. He, H. Zhuang, H. Li, N. Li, Q. Xu, D. Chen, and J. Lu, Adv. Funct. Mater. **26**(1), 146 (2016).
[12]A. Bandhopadhyay and A. J. Pal, J. Phys. Chem. B **107**(11), 2531 (2003).
[13]T. W. Kim, Y. Yang, F. Li, and W. L. Kwan, NPG Asia Mater. **4**(6), e18 (2012).
[14]F. L. Jakobsson, X. Crispin, M. Cölle, M. Büchel, D. M. de Leeuw, and M. Berggren, Org. Electron. **8**(5), 559 (2007).
[15]D. R. Stewart, D. A. A. Ohlberg, P. A. Beck, Y. Chen, R. S. Williams, J. O. Jeppesen, K. A. Nielsen, and J. F. Stoddart, Nano Lett. **4**(1), 133 (2004).